TITLE PAGE

Title: Brain magnetic resonance spectroscopy in episodic hepatic encephalopathy

Running title: Brain MR Spectroscopy in episodic HE

Authors:

Laia Chavarria[1,2,3], Juli Alonso[2,4], Rita García-Martínez[1], Macarena Simón-Talero[1,3], Meritxell Ventura[1,3], Clara Ramírez[5], Maria Torrens[1], Víctor Vargas[1,2,3], Alex Rovira [4], Juan Cordoba[1,2,3]

Affiliations:

1. Liver Unit, Hospital Vall d'Hebron, Barcelona, Spain
2. Centro de Investigación Biomédica en Red de Enfermedades Hepáticas y Digestivas (CIBEREHD), Instituto de Salud Carlos III, Madrid, Spain
3. Departament de Medicina, Universitat Autònoma de Barcelona, Bellaterra, Spain
4. Magnetic Resonance Unit (IDI), Department of Radiology, Hospital d'Vall Hebron, Barcelona, Spain
5. Biochemistry Unit, Hospital Vall d'Hebron, Barcelona, Spain

Author addresses:

Laia Chavarria: laia.chavarria@vhir.org

Juli Alonso: juli.alonso@idi-cat.org

Rita García-Martínez: humrita77@yahoo.es

Macarena Simón-Talero: ms-talero@hotmail.com

Meritxell Ventura-Cots: txell.ventura.cots@gmail.com

Clara Ramírez: clramirez@vhebron.net

Maria Torrens: mariacadaques@hotmail.com

Víctor Vargas: vvargas@vhebron.net

Alex Rovira: alex.rovira@idi-cat.org

Joan Córdoba: jcordoba@vhebron.net

Grant Support:

This project was supported by grant from Instituto de Salud Carlos III (FIS PI07/0641 and PI08/0698) cofinanced by the European Regional Development Fund (ERDF). CIBEREHD is supported by *Instituto de Salud Carlos III*. Rita Garcia-Martinez is the recipient of grant CM07/00109.

Contact Information:

Juan Córdoba Cardona
Hospital Universitari Vall d'Hebron
Passeig Vall d'Hebron 119-129
08035 Barcelona, Spain
Email:jcordoba@vhebron.net
Tel: +34 932476140
Fax: +34 932476068

Disclosures

Nothing to disclose

Abbreviation Key:

HE: hepatic encephalopathy

MR: magnetic resonance

ADC: apparent diffusion coefficient

FLAIR: fluid attenuated inversion recovery

TR: repetition time

TE: echo time

TI: inversion time

Ins: myo-inositol

Glx: glutamine and glutamate

Gln: glutamine

Glu: glutamate

NAA: N-acetylaspartate

Cr: creatine

ABSTRACT

Brain magnetic resonance (MR) has shown metabolic abnormalities and changes in the distribution of water that may relate to the pathogenesis of hepatic encephalopathy (HE). We designed a study to investigate the disturbances of brain water and metabolites during episodic HE using a 3T-MR scanner.

Cirrhotic patients with different grades of HE at the time of admission underwent MR during hospitalization (n=18). MR was repeated at six weeks (n=14). The results were compared with those of a group of healthy voluntaries (n=8). During episodic HE, brain diffusion weighted imaging shows a high apparent diffusion coefficient (ADC) that decreases during follow-up. These disturbances were accompanied by high glutamine, low choline and low myoinositol (MR-spectroscopy). In overt encephalopathy patients showed higher glutamine that decreased during follow up. In addition, patients exhibited a rise in plasma S100 beta and an enlargement of brain white matter lesions.

In conclusion, several disturbances detected by MR support the presence of impaired brain water homeostasis during episodic HE. In spite of the major role of the astrocyte in HE, brain edema during episodic HE is mostly extracellular and does not appear to be directly responsible for the development of neurological manifestations.

Keywords:

Acute hepatic encephalopathy, blood-brain-barrier, glutamine, leukoaraiosis, spectroscopy

INTRODUCTION

Hepatic encephalopathy (HE) is a common complication of cirrhosis that covers a wide range of neurological manifestations, from subtle cognitive deficits to deep coma (1). Current hypothesis on the pathogenesis of HE are focused on the impairment of astrocyte function (2), which determines the integrity of the blood-brain-barrier (BBB), the concentration of neurotransmitters in the synaptic cleft and the energetic supply to the neuron. It has been postulated that ammonia and neuroinflammation induce astrocyte swelling (3), which may result in increased BBB permeability to some molecules (4) and in neuronal dysfunction (5).

MR methods allow studying brain water and metabolites in patients with liver failure (6). Water quantification has demonstrated a trend towards higher proportion of water in the white matter in mild HE (7). This finding is compatible with the results of studies using magnetization transfer, which show indirectly the accumulation of water in the brain (8). However, contrary to what should be expected from the hypothesis of edema secondary to astrocyte swelling, diffusion weighted imaging in cirrhosis indicate that the increase of water is located in the extracellular compartment (9). Analysis of diffusion imaging using a biexponential approach (in contrast to the standard monoexponential analysis) supports the presence of two components of two components that can be ascribed to water bounded to membranes (mostly intracellular) or unbounded to membranes (mostly extracellular). Although the interpretation is controversial, the results of applying this method to patients with cirrhosis are in accordance with an increase of water in the extracellular compartment (10).

A possible explanation for the discrepancies among different studies is that the distribution of brain edema among different compartments depends on the temporal course of liver injury. Experimentally induced hyper-acute liver failure causes intracellular brain swelling (low ADC) without affecting the permeability of the BBB (11), but sub-acute models are characterized by a mixed pattern of cytotoxic (intracellular) and vasogenic (extracellular) edema (12). Similarly, ADC values are low in patients with acute liver failure (cytotoxic edema) (13) and unaffected in acute-on-chronic liver failure (mixed vasogenic and cytotoxic edema) (14). HE is much more frequently associated with cirrhosis than with acute or acute-on-chronic liver failure. However, most MR studies have been performed in patients with cirrhosis and minimal HE and few studies have controlled for individual variables by reassessing the same patient after the recovery of HE (15). The metabolic profile detected by MR spectroscopy in 1.5 T equipments is characterized by an increase in the Glx peak (which can not separate glutamate and glutamine) and a decrease in myo-inositol and choline derivates (16-18). This pattern has been attributed to the induction of elevated intracellular osmolality secondary to the metabolism of ammonia to glutamine, and the compensatory release of organic osmolytes (myo-inositol and glycerophosphocholine) from the astrocyte to the extracellular space.

The aim of the study was to investigate the disturbances of brain water and metabolites and relate them to the course of HE. MR was performed with a 3T-scanner, which allows assessing brain glutamine (19), a key factor in ammonia-related neurotoxicity (20). The findings could support current pathogenic hypothesis and may be useful for developing diagnostic biomarkers. In

addition, we assessed the concentration of astroglial protein S100 beta in serum, which is known to indicate glial injury and BBB dysfunction (21;22).

MATERIAL AND METHODS

Design

The study consisted in a prospective assessment of clinical and MR characteristics of a group of patients with cirrhosis that were admitted to the hospital because of an episode of overt HE. The patients were clinically stable, without manifestations of neurological impairment before the episode of HE (within 5 days before admission). All patients underwent daily biochemical analysis, clinical evaluation and assessment of the grade of HE (twice a day) until MR exam (within the first 5 days of admission). The grade of HE was determined within 30 minutes of MR assessment. The study was repeated after six weeks (±1 week) in 14 patients that recovered from HE (2 patients died and 2 patients rejected the second MR. At the time of the second MR most patients did not exhibit clinical signs of HE, but 2 patients still exhibited HE grade 1. The Ethics Committee of Hospital Universitari Vall d'Hebron approved the study and an informed consent was obtained from participants (first by next of kin and later confirmed by the patient).

Patient characteristics

The study included eighteen patients that showed at admission signs of overt HE (grade II [n=6], grade III [n=10] and grade IV [n=2]). All of them exhibited typical clinical and biochemical parameters of cirrhosis (table 1), that did not differ in relation to the severity of HE (supplementary table 1). They were treated according to a standard protocol that included the correction of precipitating factors, the administration of intravenous solutions and initiation of intake of food when possible. The precipitant factors corresponded to infection

(n=5), hyponatremia (serum sodium < 130 mEq /L, n=6) and diuretic-induced dehydration (n=9). The latter was defined as the lack of edema and ascites and loss of weight (> 5 kg), less than one month after starting therapy with diuretics. All the patients received lactulose (through rectal, nasogastric or oral route) and rifaximin 600 mg bid (nasogastric or oral route). Many of them showed an improvement of HE during the first days of admission. For this reason, the grades of HE were lower at the time of MR exam: 7 patients recovered consciousness and did not show HE, 8 patients exhibited low-grade HE (grade I-II) and 3 patients high-grade HE (grade III-IV). Eight healthy voluntaries (4 male, 4 female), age-matched (57±8 years) with patients were evaluated as control group.

Analytical procedures

Standard laboratory test included: hemogram, reticulocytes count, prothrombine time, bilirubin, ALT, AST, alkaline phosphatase, albumin, sodium, potassium, creatinine and calcium. Ammonia was measured in a Cobas Integra analyzer (Roche Diagnostics Indianapolis, IN, USA) by standard methodology. The serum S100 beta protein levels were measured using an electrochemiluminescence immunoassay (ECLIA) for use on Eclecsys immunoassay system (Roche Diagnostics, Switzerland). The results of the concentration of S100 beta are given in µg/L (95^{th} percentile value of apparently heathy persons is 0.105 µg/L). The immunoassay is unaffected by icterus (bilirubin < 25mg/dL) and hemolysis (hemoglobin < 1g/dL). The eighteen patients had bilirubin levels below the limits of interference; however, two of them had hemolytic samples and were not considered for analysis.

MR protocol

MR studies were performed in a 3.0T MAGNETOM Trio scanner (Siemens, Erlangen, Germany) equipped with a circular polarized receiver head array coil with the body coil acting as transmitter.

The MR protocol included proton density and T2-weighted fast spin-echo (repetition time [TR] /echo time [TE]/echo train length/acquisitions/ turbo factor [FT] 2900 ms /19 -87 ms/16/2/6) and fast-FLAIR (TR /TE /inversion time [TI] / echo train length/acquisitions/FT 9000 ms/93 ms/2500 ms/12 /1/16). Forty-six contiguous axial slices with a thickness of 3mm, a pixel size of approximately 1x1mm, a 3/4 rectangular field of view of 250mm, and an acquisition matrix of 256x256 were used to record images. T1-weighted images were obtaining using magnetization-prepared 180º radio-frequency pulses and rapid gradient-echo (TR /TE /TI / acquisitions 2700 ms/ 4.32 ms/ 900 ms/ 1). A total of 176 contiguous sagital slices with a thickness of 1mm, a pixel size of approximately 1x1 mm, a field of view of 256mm and an acquisition matrix of 256x256 were applied to obtain images.

Diffusion images were acquired using a single-shot echo-planar sequence (TR/TE/acquisitions/FT 4000ms/93ms/6/128) with gradients applied in three directions and four b-values (range 0-3000s/mm^2). Images were obtained in 28 axial slices with a slice thickness of 4mm, an interslice gap of 2mm, a field of view of 250mm, and an acquisition matrix of 128x128.

Proton MR spectroscopy was performed from a volume of interest localized at the parieto-occipital region and defined by a cube of 20mm side containing mainly white matter. A 90º-180º-180º spin-echo–based pulse sequence was

used (TR /TE /acquisitions 3000ms /30ms /80). For water suppression, a chemical shift selective Gaussian pulse was applied. A total of 1024 data points were collected over a bandwith of 1200Hz.

MR analysis

All fast-FLAIR images obtained at baseline and follow-up scans were used to identify T2 lesion. These lesions were marked on MR plates and only focal white matter lesions located in the brain hemispheres and at least 3mm in size were considered for the measurement. Then, lesions marked on MR plates were outlined on the computer image to compute the lesion surface using the Jim image analysis package (version 5.0, Xinapse Systems Ltd, Northants, UK, www.xinapse.com).

Diffusion imaging data were processed using NUMARIS4 software syngo version (Siemens, Erlangen, Germany) to calculate apparent diffusion coefficient (ADC; in $\mu m^2/s$) in two regions: parietal white matter and corticospinal tract.

Spectra were analyzed using LCModel software v6.2-4A (Stephen Provencher Inc, Oakville, ON, Canada) to quantify automatically the metabolites (ratios compared to creatine [Cr]) without water scaling (23) (supplementary figure 1). Glutamine, glutamate, compounds of NAA (N-acetylaspartate and N-acetylaspartylglutamate), choline derivates (glycerophosphorylcholine and phosphorylcholine) and myo-inosiyol were analyzed by fitting a linear combination of a basis set of metabolite model spectra to the data (LCModel). The basis set was simulated using the GAMMA library.

Statistical analysis

The statistical analysis was performed with Sigma Stat package (SPSS Inc, Chicago, USA). Values are expressed as the mean ± standard deviation. Significant differences between intergroup data were verified with the Student's t-test, Mann-Whitney U test or ANOVA. ANOVA test were followed by all pairwise multiple comparison procedures (Holm-Sidak method or Dunn's Method). The comparisons between continuous variables were carried out with the paired Student's t-test or Wilcoxon W test. The correlations between parameters were performed with Pearson or Spearman's correlation. P-values <0.050 were considered statistically significant.

RESULTS

The metabolic profiles obtained by spectroscopy were abnormal in patients with cirrhosis compared to controls: a) glutamine was higher (Gln/Cr: 2.40±0.78 vs 0.22±0.08, P<0.001) and b) myo-inositol and choline derivates were lower (Ins/Cr: 0.14±0.07 vs 0.66±0.07, P<0.001; Cho/Cr: 0.20±0.04 vs 0.26±0.03, P=0.002). However, glutamate and N-acetylaspartate were not significantly different (Glu/Cr: 1.10±0.20 vs 1.06±0.08, P=0.157 and NAA/Cr: 1.77±0.02 vs 1.64±0.08, P=0.92). The peak of glutamine increased significantly in relation to the severity of HE (P=0.038), while the peak of choline derivates exhibited a decrease (P=0.048) (figure 1a). There was a positive correlation between glutamine/creatine ratio and HE grade (r=0.608, P=0.007) (figure 1b). During the follow-up the peak of glutamine decreased ~36 % in those patients that recovered from the episode of HE (from 2.42±0.65 to 1.55±0.55, P=0.028). In contrast, glutamine remained stable in those patients that were admitted to the hospital showing HE, but exhibited normal mental status at MR assessment (baseline: 2.03±0.65, six weeks: 1.94±0.66, P = 0.663) (figure 2). Brain glutamine correlated to blood ammonia in the group of 14 patients with baseline and follow-up data (r=0.526, P=0.004, n=28). Myo-inositol increased in the follow-up (baseline: 0.14±0.07, follow-up: 0.21±0.09, P=0.006), but there was no relation with the severity of HE. The changes in glutamine during follow-up did not correlate with the changes in myo-inositol (r= -0.179, P= 0.579). Other metabolites (glutamate, choline and N-acetylaspartate) remained stable. The same analysis was performed using absolute signal for each metabolite and statistical differences were maintained. In addition, absolute signal of creatine did not differ between controls and patients (supplementary table 2).

In patients with cirrhosis diffusion weighted imaging showed that ADC values were higher in the corticospinal tract (804±66 $\mu m^2/s$ vs 707±29 $\mu m^2/s$; P < 0.001) and in the parietal white matter (895±67 $\mu m^2/s$ vs: 798± 57 $\mu m^2/s$; P = 0.005) compared to controls. The increase in ADC values tended to be higher in relation to the severity of HE (figure 3a), reaching statistical significance in the corticospinal tract (P = 0.006). In the follow-up, ADC values (in the twelve patients who recovered from the HE episode) exhibited a significant decrease in the corticospinal tract (from 780±44 $\mu m^2/s$ to 758±44 $\mu m^2/s$, P=0.025) and in the parietal white matter (from 884±54 $\mu m^2/s$ to 842±38 $\mu m^2/s$, P=0.016) (figure 3b). The ADC values in parietal white matter in the follow-up did not differ from controls. However, ADC values of patients persisted slightly elevated in the corticospinal tract.

Fifteen patients exhibited T2 focal lesion in the white matter, of whom nine were revaluated after HE resolution. The lesion volume diminished after the episode of HE (P=0.039) (figure 4). The comparison between precipitating factors and MR parameters at baseline showed that ADC values in parietal white matter were higher in dehydration (no-dehydrated= 861±44 $\mu m^2/s$ vs dehydrated= 928±70 $\mu m^2/s$; P=0.027). In addition, myo-inositol/creatine ratio was lower in patients with hyponatremia (0.092±0.05 vs 0.16±0.07; P=0.031).

The concentration of serum S100 beta correlated at baseline with the grade of HE (r=0.584, P=0.018, n=16) (figure 5), but was not associated with other clinical or MR variables.

DISCUSSION

The study shows abnormalities in the amount of several metabolites and in the distribution of water in brain compartments in episodic HE. Some of these disturbances, specifically brain glutamine, appear to be of pathogenic relevance and may be useful for the diagnosis of HE.

Liver failure secondary to cirrhosis impairs the capacity to transform ammonia into urea, which is the metabolite that disposes nitrogenous molecules from the body in normal conditions. In cirrhosis, plasma ammonia increases and in conjunction with inflammatory mediators can result toxic to the brain and precipitate the development of neurological manifestations (HE). Ammonia reaches the BBB and is rapidly metabolized to glutamine in the astrocytes, which are part of the BBB (1). Glutamine has been classically considered an inert amino acid, but has been proposed to be *toxic* to the astrocyte trough acting as a carrier of ammonia to the interior of the mitochondria (20). Glutamine accumulation could be also related to the diminished capacity of astrocytes to take up glutamate thus leading to glutamate excitotoxicity (24). Alternatively, it may be simply an indicator of the exposure of the brain to ammonia, which may be the key factor in the development of HE. We observed a high rise in brain glutamine (10 fold compared to controls), which is in the order observed in experimental models (11;25). The rise in baseline glutamine was more marked in those patients with more severe forms of HE (grade III-IV). Unfortunately, we were not able to reassess glutamine in the follow-up of patients with severe HE. Nevertheless, those with mild HE (grade I-II) at baseline showed a decrease in glutamine of more than one third during recovery (grade 0). In comparison, glutamine remained stable in those without

HE at the time of performing MR, with values similar to those obtained at follow-up in the mild HE group that recovered normal mental status. Other studies have also found an increase in the peak of glutamine in overt HE (26) and a tendency to decrease with therapy for HE (27). Probably, according to our data, the lack of significant decrease in Glx in previous studies (15) relates to insufficient resolution of 1.5T equipments.

Irrespective of its role in the pathogenesis of HE, the assessment of glutamine by MR-spectroscopy could be an useful biomarker in the diagnosis of difficult cases. Cirrhotic patients may develop non-hepatic encephalopathy secondary to small-vessel cerebrovascular disease or Alzheimer's disease; MR-spectroscopy can help in the diagnosis of these cases. Although glutamine values overlapped between different grades of HE, in our hands its evolution were related closely to the evolution of HE. For this reason, alternative diagnosis to HE should be suspected in those cases that show discrepancies between the evolution of brain glutamine and the evolution of neurological manifestations. Further studies are necessary to confirm this hypothesis.

The most important mechanism by which brain glutamine has been proposed to originate HE is by inducing astrocyte swelling and impairing its function (28). The observation of a decrease in ADC in patients with acute liver failure supports this interpretation (29). However, MR studies in patients with cirrhosis have consistently found a rise in ADC. Others studies in clinical situations where brain edema is extracellular (brain tumors, hypernatremia) have found an increase in ADC, while in patients with intracellular edema (hyponatremia) ADC has been shown to decrease (30;31). These findings are contrary to the hypothesis that the severity of HE is directly caused by astrocyte swelling. Our

data show the lack of relationship between neurological manifestations and the distribution of water between the intracellular and extracellular compartment (9;32). We found an increase in the ADC that represents an expansion of the extracellular compartment that returned to normal in the follow-up in parietal white matter. Similarly to a previous study that assessed ADC in the corticospinal tract before and after liver transplant, ADC in the spine did not completely normalized after recovery of HE (10), which can be explained by persisting neurological damage (mild hepatic myelopathy) (33).These results suggest a higher vulnerability of the corticospinal tract for developing liver-induced damage.

ADC was higher in patients with signs of body dehydration. This is an intriguing finding that may be explained by the inhibition of water transport across the BBB caused by diuretics (the main cause of dehydration) (34). Interestingly, diuretics are a frequent factor associated with episodic HE, to which no mechanistic explanation has been found. The association between low brain myo-inositol and hyponatremia seen in our and other studies (35) is an additional sign of disturbance of brain water homeostasis. Myo-inositol has an important role in the brain as an osmotic osmolyte that increases or decreases its concentration in astrocytes to equilibrate changes in extracellular osmolalilty (36). The decrease in myo-inositol has been proposed to compensate for an increase in astrocyte osmolality caused by the synthesis of glutamine from ammonia. Lack of osmotic compensation can cause an increase in the amount of water in the astrocyte and explain the development of neurological manifestations. However, we could not relate ADC values nor myo-inositol to

the severity of HE, suggesting that HE cannot simply be attributed to brain edema.

Our findings are not contrary to the participation of the astrocyte in the pathogenesis of HE. One possible explanation to reconcile our data with signs of glial injury seen in HE is the participation of the astrocyte in the blood-brain-barrier. White matter lesions in T2-weighted images compatible with small-vessel cerebrovascular disease were observed in an important proportion of our patients (37). Recent studies have shown that these lesions are probably indicative of higher permeability of the blood-brain-barrier (38;39). It is plausible that during HE, ammonia or glutamine cause an impairment of the astrocyte function, as supported by the association between the severity of HE and an increase in serum S100 beta. Astrocyte dysfunction could have two effects that are not directly related: brain edema and neuronal dysfunction. Improvement of astrocyte function with therapy may decrease brain edema and explain the decrease in the volume of white matter lesions and normalization of ADC (28), but some sequels in neuronal function may persist (40).

In conclusion, MR spectroscopy with 3T equipments supports the participation of brain glutamine in the pathogenesis of HE. In spite of the major role of the astrocyte, brain edema is mostly extracellular and does not appear to be directly responsible for the development of neurological manifestations. For this reason, studies on the pathogenesis of HE should avoid the use of water disturbances as a surrogate of neurological manifestations and separate brain edema and hepatic encephalopathy.

The supplementary material is available at the JCBFM web site.

REFERENCES

(1) Cordoba J, Minguez B. Hepatic encephalopathy. Semin Liver Dis 2008 Feb;28(1):70-80.

(2) Norenberg MD. Astroglial dysfunction in hepatic encephalopathy. Metab Brain Dis 1998 Dec;13(4):319-35.

(3) Zemtsova I, Gorg B, Keitel V, Bidmon HJ, Schror K, Haussinger D. Microglia activation in hepatic encephalopathy in rats and humans. Hepatology 2011 Jul;54(1):204-15.

(4) Nguyen JH, Yamamoto S, Steers J, Sevlever D, Lin W, Shimojima N, et al. Matrix metalloproteinase-9 contributes to brain extravasation and edema in fulminant hepatic failure mice. J Hepatol 2006 Jun;44(6):1105-14.

(5) Palomero-Gallagher N, Bidmon HJ, Cremer M, Schleicher A, Kircheis G, Reifenberger G, et al. Neurotransmitter receptor imbalances in motor cortex and basal ganglia in hepatic encephalopathy. Cell Physiol Biochem 2009;24(3-4):291-306.

(6) Mardini H, Smith FE, Record CO, Blamire AM. Magnetic resonance quantification of water and metabolites in the brain of cirrhotics following induced hyperammonaemia. J Hepatol 2011 Jun;54(6):1154-60.

(7) Shah NJ, Neeb H, Kircheis G, Engels P, Haussinger D, Zilles K. Quantitative cerebral water content mapping in hepatic encephalopathy. Neuroimage 2008 Jul 1;41(3):706-17.

(8) Miese FR, Wittsack HJ, Kircheis G, Holstein A, Mathys C, Modder U, et al. Voxel-based analyses of magnetization transfer imaging of the brain in hepatic encephalopathy. World J Gastroenterol 2009 Nov 7;15(41):5157-64.

(9) Lodi R, Tonon C, Stracciari A, Weiger M, Camaggi V, Iotti S, et al. Diffusion MRI shows increased water apparent diffusion coefficient in the brains of cirrhotics. Neurology 2004 Mar 9;62(5):762-6.

(10) Chavarria L, Alonso J, Garcia-Martinez R, Aymerich FX, Huerga E, Jacas C, et al. Biexponential analysis of diffusion-tensor imaging of the brain in patients with cirrhosis before and after liver transplantation. AJNR Am J Neuroradiol 2011 Sep;32(8):1510-7.

(11) Chavarria L, Oria M, Romero-Gimenez J, Alonso J, Lope-Piedrafita S, Cordoba J. Diffusion tensor imaging supports the cytotoxic origin of brain edema in a rat model of acute liver failure. Gastroenterology 2010 Apr;138(4):1566-73.

(12) Cauli O, Lopez-Larrubia P, Rodrigo R, Agusti A, Boix J, Nieto-Charques L, et al. Brain region-selective mechanisms contribute to the progression

of cerebral alterations in acute liver failure in rats. Gastroenterology 2011 Feb;140(2):638-45.

(13) Saksena S, Rai V, Saraswat VA, Rathore RS, Purwar A, Kumar M, et al. Cerebral diffusion tensor imaging and in vivo proton magnetic resonance spectroscopy in patients with fulminant hepatic failure. J Gastroenterol Hepatol 2008 Jul;23(7 Pt 2):e111-e119.

(14) Nath K, Saraswat VA, Krishna YR, Thomas MA, Rathore RK, Pandey CM, et al. Quantification of cerebral edema on diffusion tensor imaging in acute-on-chronic liver failure. NMR Biomed 2008 Aug;21(7):713-22.

(15) Poveda MJ, Bernabeu A, Concepcion L, Roa E, de ME, Zapater P, et al. Brain edema dynamics in patients with overt hepatic encephalopathy A magnetic resonance imaging study. Neuroimage 2010 Aug 15;52(2):481-7.

(16) Cordoba J, Alonso J, Rovira A, Jacas C, Sanpedro F, Castells L, et al. The development of low-grade cerebral edema in cirrhosis is supported by the evolution of (1)H-magnetic resonance abnormalities after liver transplantation. J Hepatol 2001 Nov;35(5):598-604.

(17) Tarasow E, Panasiuk A, Siergiejczyk L, Orzechowska-Bobkiewicz A, Lewszuk A, Walecki J, et al. MR and 1H MR spectroscopy of the brain in patients with liver cirrhosis and early stages of hepatic encephalopathy. Hepatogastroenterology 2003 Nov;50(54):2149-53.

(18) Verma A, Saraswat VA, Radha KY, Nath K, Thomas MA, Gupta RK. In vivo 1H magnetic resonance spectroscopy-derived metabolite variations between acute-on-chronic liver failure and acute liver failure. Liver Int 2008 Sep;28(8):1095-103.

(19) Sawara K, Kato A, Yoshioka Y, Suzuki K. Brain glutamine and glutamate levels in patients with liver cirrhosis: assessed by 3.0-T MRS. Hepatol Res 2004 Sep;30(1):18-23.

(20) Albrecht J, Norenberg MD. Glutamine: a Trojan horse in ammonia neurotoxicity. Hepatology 2006 Oct;44(4):788-94.

(21) Kanner AA, Marchi N, Fazio V, Mayberg MR, Koltz MT, Siomin V, et al. Serum S100beta: a noninvasive marker of blood-brain barrier function and brain lesions. Cancer 2003 Jun 1;97(11):2806-13.

(22) Kapural M, Krizanac-Bengez L, Barnett G, Perl J, Masaryk T, Apollo D, et al. Serum S-100beta as a possible marker of blood-brain barrier disruption. Brain Res 2002 Jun 14;940(1-2):102-4.

(23) Provencher SW. Estimation of metabolite concentrations from localized in vivo proton NMR spectra. Magn Reson Med 1993 Dec;30(6):672-9.

(24) Lemberg A, Fernandez MA. Hepatic encephalopathy, ammonia, glutamate, glutamine and oxidative stress. Ann Hepatol 2009 Apr;8(2):95-102.

(25) Cordoba J, Gottstein J, Blei AT. Glutamine, myo-inositol, and organic brain osmolytes after portocaval anastomosis in the rat: implications for ammonia-induced brain edema. Hepatology 1996 Oct;24(4):919-23.

(26) Laubenberger J, Haussinger D, Bayer S, Gufler H, Hennig J, Langer M. Proton magnetic resonance spectroscopy of the brain in symptomatic and asymptomatic patients with liver cirrhosis. Gastroenterology 1997 May;112(5):1610-6.

(27) Haseler LJ, Sibbitt WL, Jr., Mojtahedzadeh HN, Reddy S, Agarwal VP, McCarthy DM. Proton MR spectroscopic measurement of neurometabolites in hepatic encephalopathy during oral lactulose therapy. AJNR Am J Neuroradiol 1998 Oct;19(9):1681-6.

(28) Haussinger D, Kircheis G, Fischer R, Schliess F, vom DS. Hepatic encephalopathy in chronic liver disease: a clinical manifestation of astrocyte swelling and low-grade cerebral edema? J Hepatol 2000 Jun;32(6):1035-8.

(29) Rai V, Nath K, Saraswat VA, Purwar A, Rathore RK, Gupta RK. Measurement of cytotoxic and interstitial components of cerebral edema in acute hepatic failure by diffusion tensor imaging. J Magn Reson Imaging 2008 Aug;28(2):334-41.

(30) Brugieres P, Thomas P, Maraval A, Hosseini H, Combes C, Chafiq A, et al. Water diffusion compartmentation at high b values in ischemic human brain. AJNR Am J Neuroradiol 2004 May;25(5):692-8.

(31) Schwarcz A, Ursprung Z, Berente Z, Bogner P, Kotek G, Meric P, et al. In vivo brain edema classification: New insight offered by large b-value diffusion-weighted MR imaging. J Magn Reson Imaging 2007 Jan;25(1):26-31.

(32) Kale RA, Gupta RK, Saraswat VA, Hasan KM, Trivedi R, Mishra AM, et al. Demonstration of interstitial cerebral edema with diffusion tensor MR imaging in type C hepatic encephalopathy. Hepatology 2006 Apr;43(4):698-706.

(33) Weissenborn K, Tietge UJ, Bokemeyer M, Mohammadi B, Bode U, Manns MP, et al. Liver transplantation improves hepatic myelopathy: evidence by three cases. Gastroenterology 2003 Feb;124(2):346-51.

(34) Jayakumar AR, Valdes V, Norenberg MD. The Na-K-Cl cotransporter in the brain edema of acute liver failure. J Hepatol 2011 Feb;54(2):272-8.

(35) Guevara M, Baccaro ME, Torre A, Gomez-Anson B, Rios J, Torres F, et al. Hyponatremia is a risk factor of hepatic encephalopathy in patients

with cirrhosis: a prospective study with time-dependent analysis. Am J Gastroenterol 2009 Jun;104(6):1382-9.

(36) McManus ML, Churchwell KB, Strange K. Regulation of cell volume in health and disease. N Engl J Med 1995 Nov 9;333(19):1260-6.

(37) Minguez B, Rovira A, Alonso J, Cordoba J. Decrease in the volume of white matter lesions with improvement of hepatic encephalopathy. AJNR Am J Neuroradiol 2007 Sep;28(8):1499-500.

(38) Fernandez-Cadenas I, Mendioroz M, Domingues-Montanari S, Del Rio-Espinola A, Delgado P, Ruiz A, et al. Leukoaraiosis is associated with genes regulating blood-brain barrier homeostasis in ischaemic stroke patients. Eur J Neurol 2011 Jun;18(6):826-35.

(39) Topakian R, Barrick TR, Howe FA, Markus HS. Blood-brain barrier permeability is increased in normal-appearing white matter in patients with lacunar stroke and leucoaraiosis. J Neurol Neurosurg Psychiatry 2010 Feb;81(2):192-7.

(40) Bajaj JS, Schubert CM, Heuman DM, Wade JB, Gibson DP, Topaz A, et al. Persistence of cognitive impairment after resolution of overt hepatic encephalopathy. Gastroenterology 2010 Jun;138(7):2332-40.

FIGURE LEGENDS

Figure 1: a) Relative metabolic concentration in patients with cirrhosis (n=18) and healthy control (n=8). Metabolites: Gln, glutamine; Glu, glutamate Ins, myo-inositol; Cho, choline derivates; and NAA, N-acetylaspartate. * P<0.050; b) Correlation of baseline brain glutamine/creatine ratio (Gln/Cr) and the grade of HE determined at the time of the RM exam

Figure 2: The follow-up of brain glutamine (Gln/Cr) in relation to the severity of HE at baseline. *P<0.050

Figure 3: a) Apparent diffusion coefficient values (ADC, in μm2/s) of patients with different degrees of HE (in grey, n=18) and controls (ctrl, in white, n=8) in two different regions. The mean of each group is marked by a dash. *P<0.050; b) The follow-up of apparent diffusion coefficient values (ADC, in μm2/s) of patients with cirrhosis (n=12) in two brain regions. At baseline assessment the values of patients without HE are shown as grey circles, while patients with low-grade HE (grade I-II) are shown as dark grey circles. Healthy ctrl are shown to provide a reference of the normal range. *P<0.050

Figure 4: T2 lesion volume in the 9 cirrhotic patients that exhibited white matter lesions at baseline and follow-up. *P<0.050

Figure 5: Correlation between the concentration of serum S100 beta protein levels and the grade of HE at the time of the RM exam.

Table 1: Demographic, clinical and laboratory characteristics of cirrhotic patients with acute episode of HE (baseline) and six weeks after the episode of HE (follow-up).

Study	Baseline	Follow-up
Number	18	14
Age (years)	60 ± 10	59 ± 11
Male/female	13/5	10/4
Etiology		
hepatitis C virus	2	2
alcohol	8	5
hepatitis C virus + alcohol	3	3
Other	5	4
HE grade*		
0	7	12
I	5	2
II	3	0
III	1	0
IV	2	0
Child Pugh A/B/C	1/4/2	0/5/6
Biochemical parameters**		
Prothrombin activity (%)	53.2 ± 13.9	64.0 ± 17.2
Sodium (mEq/L)	134.6 ± 6.3	136.3 ± 3.8
Potassium (mEq/L)	4.0 ± 0.6	4.4 ± 0.3
Creatinine (mg/dl)	1.1 ± 0.7	0.9 ± 0.3
Total bilirubin (mg/dl)	2.8 ± 1.0	2.2 ± 1.1
Conjugated bilirubin (mg/dl)	1.1 ± 0.4	0.9 ± 0.5
Albumin (g/dl)	3.3 ± 0.6	3.3 ± 0.4
Aspartate transaminase (UI/L)	58.6 ± 48.8	68.5 ± 59.3
Alanine transaminase (UI/L)	36.9 ± 32.3	47.7 ± 40.2
Alkaline phosphatase (UI/L)	118.8 ± 47.0	144.9 ± 74.1
gamma-Glutamyl transpeptidase (UI/L)	96.0 ± 79.1	110.2 ± 35.8
Plasma ammonia concentration (μM)	105.8 ± 53.5	89.5 ± 47.8

* West-Haven criteria. ** determined in venous samples

FIGURES:

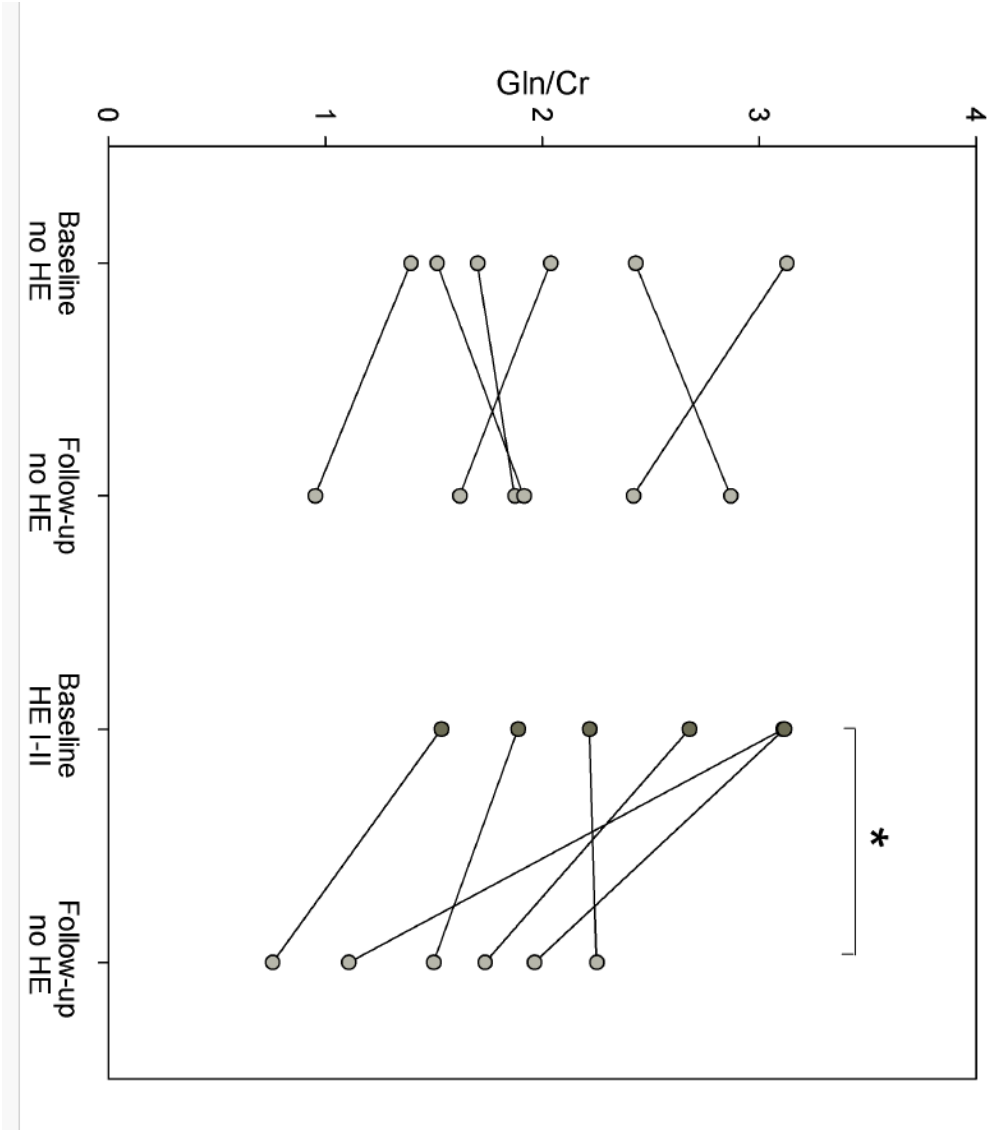
Gln/Cr
0
1
2
3
4
Baseline no HE
Follow-up no HE
Baseline HE I-II
Follow-up no HE
*

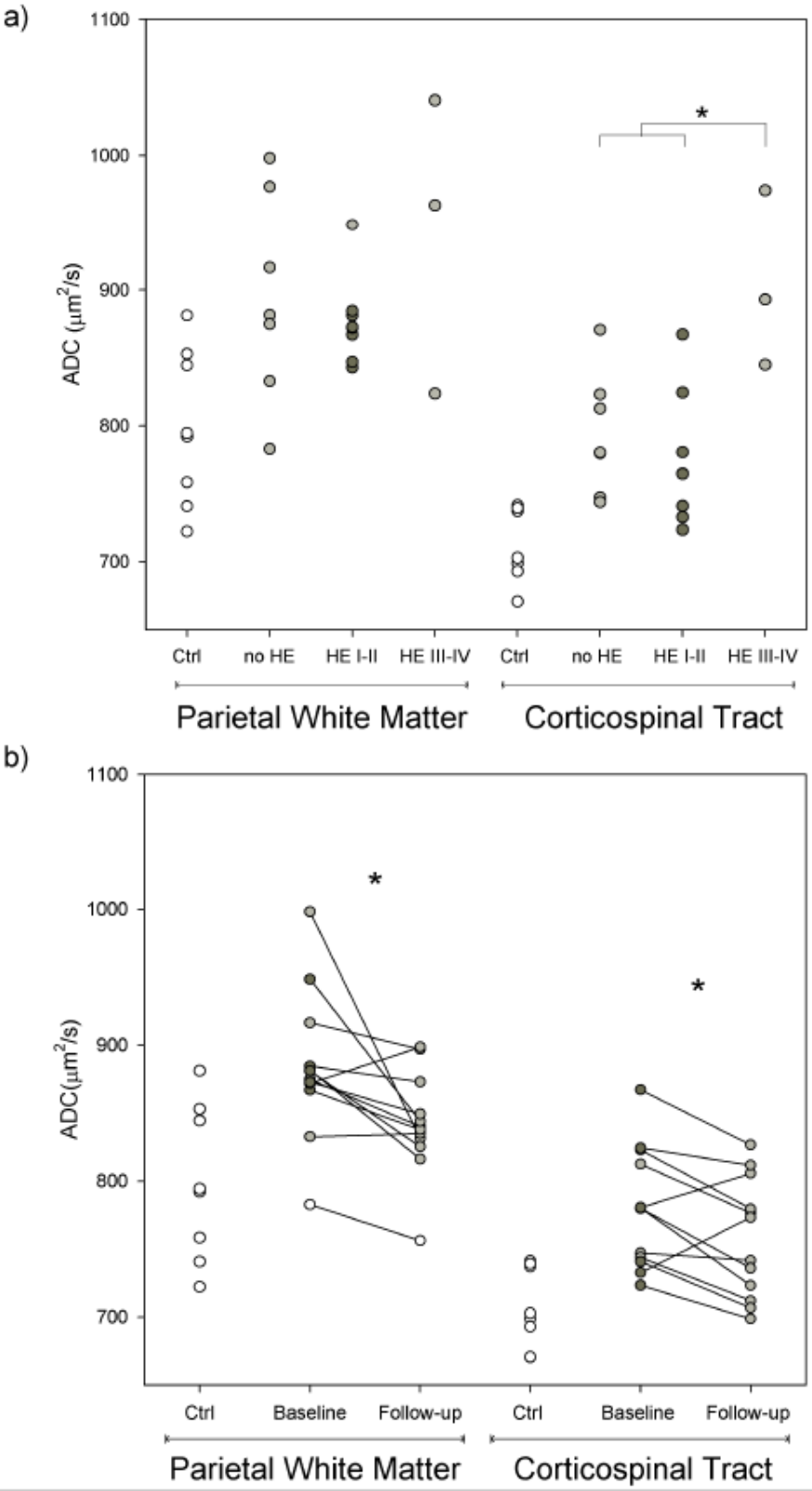
a)
1100
1000
900
800
700
ADC (μm²/s)
*
Ctrl
no HE
HE I-II
HE III-IV
Ctrl
no HE
HE I-II
HE III-IV
Parietal White Matter
Corticospinal Tract
b)
1100
1000
900
800
700
ADC(μm²/s)
*
*
Ctrl
Baseline
Follow-up
Ctrl
Baseline
Follow-up
Parietal White Matter
Corticospinal Tract

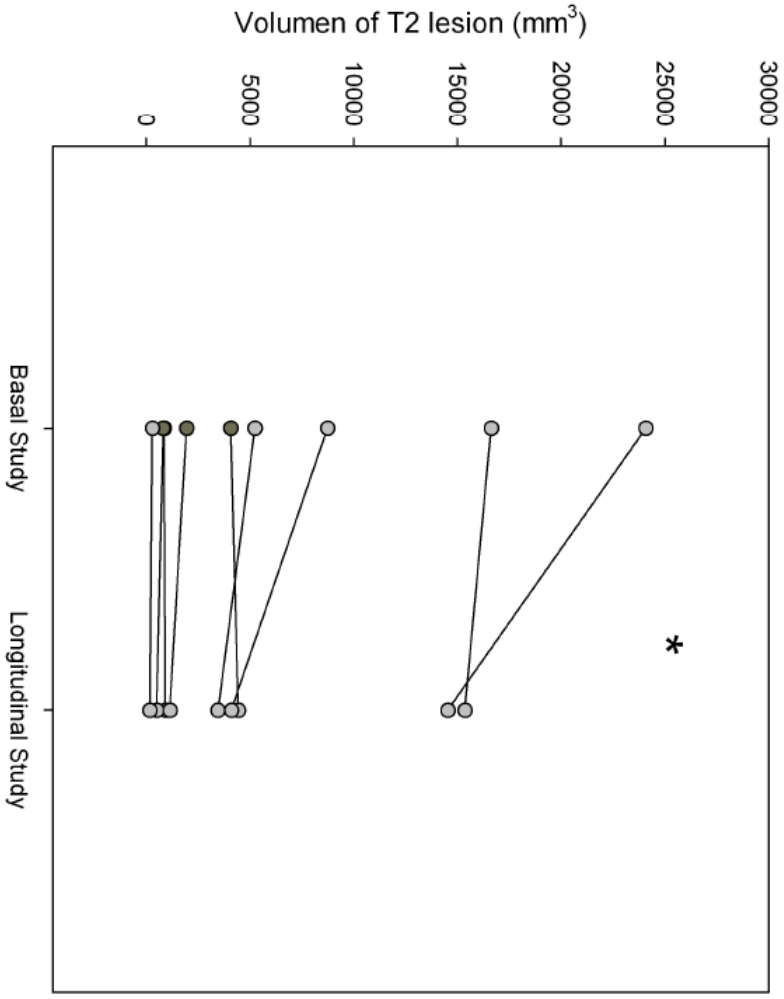
Volumen of T2 lesion (mm3)
0
5000
10000
15000
20000
25000
30000
Basal Study
Longitudinal Study
*

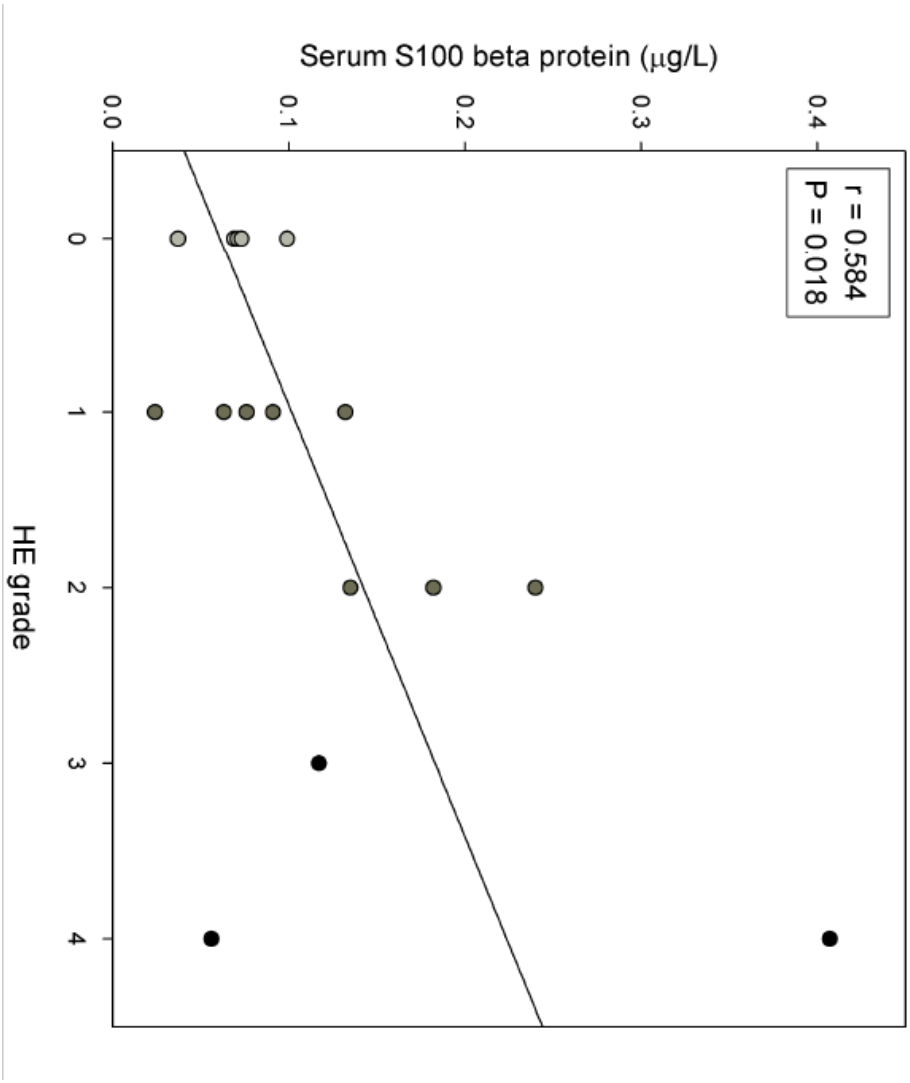
Serum S100 beta protein (μg/L)
0.0
0.1
0.2
0.3
0.4
r = 0.584
P = 0.018
HE grade
0
1
2
3
4

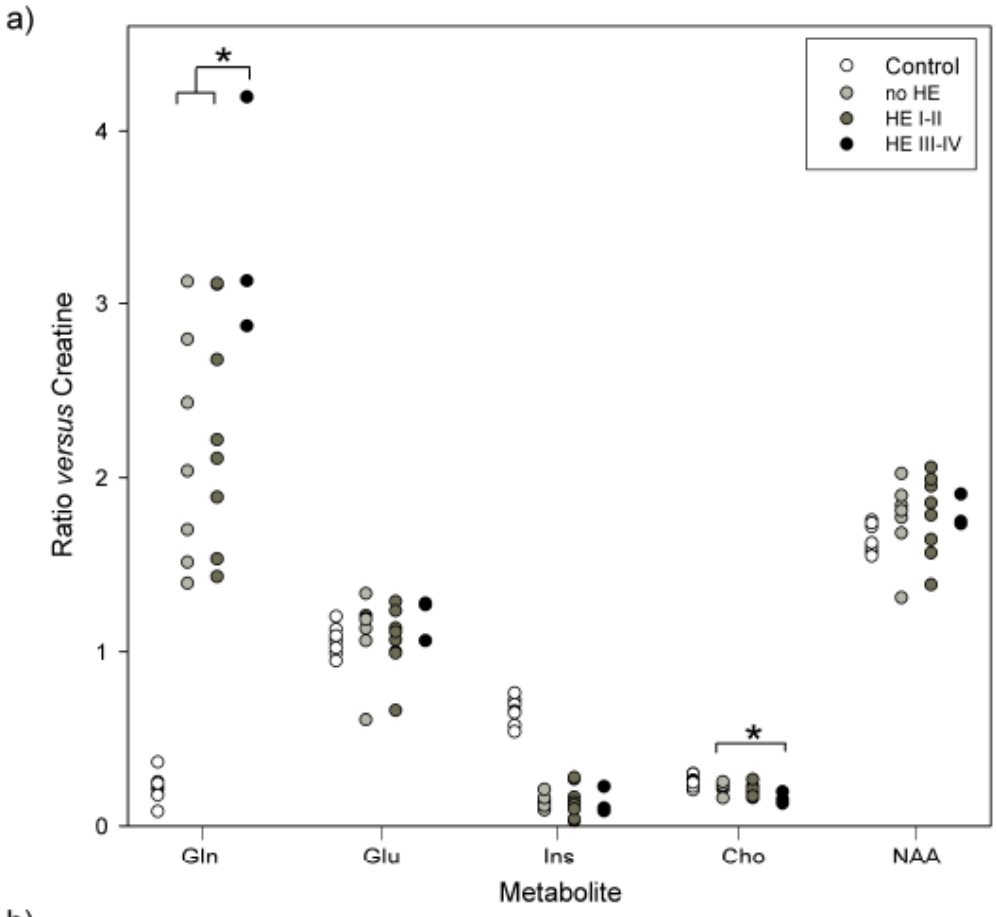
a)
Control
no HE
HE I-II
HE III-IV
*
*
Ratio versus Creatine
0
1
2
3
4
Gln
Glu
Ins
Cho
NAA
Metabolite

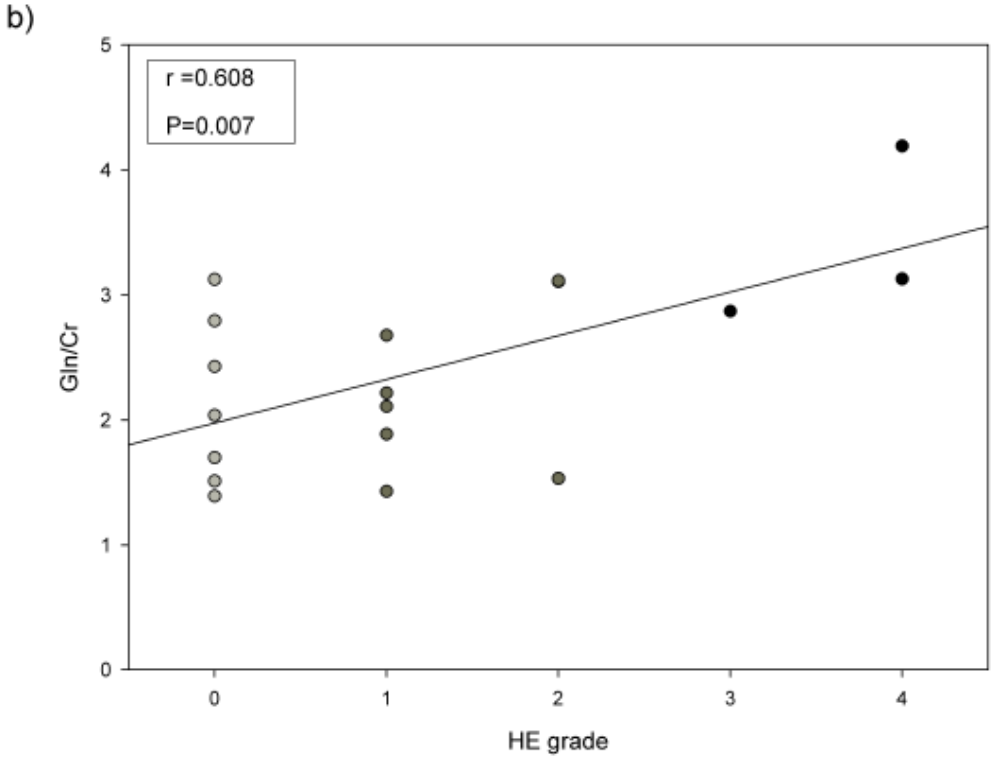
b)
r =0.608
P=0.007
Gln/Cr
0
1
2
3
4
5
0
1
2
3
4
HE grade